Astronomy & Astrophysics

IPHAS extinction distances to planetary nebulae

C. Giammanco[1,12], S. E. Sale[2], R. L. M. Corradi[1,12], M. J. Barlow[3], K. Viironen[1,13,14], L. Sabin[4],
M. Santander-García[5,1,12], D. J. Frew[6], R. Greimel[7], B. Miszalski[10], S. Phillipps[8], A. A. Zijlstra[9],
A. Mampaso[1,12], J. E. Drew[2,10], Q. A. Parker[6,11], and R. Napiwotzki[10]

[1] Instituto de Astrofísica de Canarias (IAC), C/ vía Láctea s/n, 38200 La Laguna, Spain
    e-mail: corrado@iac.es
[2] Astrophysics Group, Imperial College London, Blackett Laboratory, Prince Consort Road, London SW7 2AZ, UK
[3] Department of Physics and Astronomy, University College London, Gower Street, London WC1E 6BT, UK
[4] Instituto de Astronomía, Universidad Nacional Autónoma de México, Apdo. Postal 877, 22800 Ensenada, B.C., Mexico
[5] Isaac Newton Group of Telescopes, Ap. de Correos 321, 38700 Sta. Cruz de la Palma, Spain
[6] Department of Physics, Macquarie University, NSW 2109, Australia
[7] Institut für Physik, Karl-Franzens Universität Graz, Universitätsplatz 5, 8010 Graz, Austria
[8] Astrophysics Group, Department of Physics, Bristol University, Tyndall Avenue, Bristol BS8 1TL, UK
[9] Jodrell Bank Centre for Astrophysics, School of Physics and Astronomy, University of Manchester, Oxford Road,
    M13 9PL Manchester, UK
[10] Centre for Astrophysics Research, STRI, University of Hertfordshire, College Lane Campus, Hatfield AL10 9AB, UK
[11] Anglo-Australian Observatory, PO Box 296, Epping, NSW 1710, Australia
[12] Departamento de Astrofísica, Universidad de La Laguna, 38205 La Laguna, Tenerife, Spain
[13] Centro Astronómico Hispano Alemán, Calar Alto, C/Jesús Durbán Remón 2-2, 04004 Almeria, Spain
[14] Centro de Estudios de Física del Cosmos de Aragón (CEFCA), C/General Pizarro 1-1, 44001 Teruel, Spain

Received 19 March 2010 / Accepted 3 July 2010

ABSTRACT

Aims. The determination of reliable distances to planetary nebulae (PNe) is a major difficulty in the study of this class of objects in the Galaxy. The availability of new photometric surveys such as IPHAS (the INT/WFC photometric H_α survey of the northern Galactic plane) covering large portions of the sky provide an opportunity to apply the so-called extinction method to determine the distances of a large number of objects.
Methods. The technique is applied to a sample of 137 PNe located between −5 and 5 degrees in Galactic latitude, and between 29.52 and 215.49 degrees in longitude. The characteristics of the distance-extinction method and the main sources of errors are carefully discussed.
Results. The data on the extinction of the PNe available in the literature, complemented by new observations, allow us to determine extinction distances for 70 PNe. A comparison with statistical distance scales from different authors is presented.

Key words. catalogs – planetary nebulae: general

1. Introduction

The measurements of the distances to Galactic planetary nebulae (PNe) has been a longstanding difficulty. Obtaining an accurate distance scale for Galactic PNe will allow us to infer the total number of PNe in the Galaxy, which has important implications for the Galactic ultraviolet radiation field, the total processed mass returned to the interstellar medium, and more generally to our understanding of the chemical evolution of the Galaxy.

A method that is a priori independent of assumptions about the physical or geometrical properties of the nebulae is the extinction method. Assuming that the interstellar extinction to a certain nebula can be determined, if one is able to build up the extinction-distance relation using field stars around the line of sight to the nebula, the relation can be used to infer the distance to the planetary nebula (PN).

The application of this method is not new. Lutz (1973) measured the distance to 6 PNe using some 10 field stars per object. The method was later applied by Acker (1978) who provided reliable distance values for 11 PNe and a rough estimate for

34 other ones, and by Gathier et al. (1986) who measured the distance to 12 PNe using some 50 stars per PN. In the last paper, a comprehensive discussion of the different aspects of this method can be found. The number of stars used to determine distances was increased by Pollacco & Ramsay (1992) who, using a colour analysis of the field stars, were able to perform an accurate spectral classification for stars later than F5 type. As late-type stars constitute the most numerous objects in all Galactic-plane directions, they allow an extensive application of this method to determine distances to PNe in the Galaxy.

The availability of the IPHAS H_α survey of the northern Galactic plane (Drew et al. 2005) and its forthcoming extension to the south (VPHAS+) opens new doors for the application of the method. IPHAS allows us to determine extinction-distance curves using a large number of field stars, typically several hundred in areas as small as $10' \times 10'$ around each line of sight. The technique is presented and discussed by Sale et al. (2009). In this paper, we present its application to Galactic PNe. We determine the distances to 70 PNe included in the ESO/Strasbourg catalogue (Acker et al. 1992), and compare the distances obtained

---

with those obtained by other authors using different methods. This shows how IPHAS and its successor surveys potentially provide a new and powerful tool to obtain distances to a large number of Galactic PNe.

2. The data

IPHAS is a wide-field, CCD, Hα survey of the northern Galactic plane (Drew et al. 2005), which was carried out at the 2.5 m Isaac Newton Telescope on La Palma, Spain. Imaging was also performed in the r' and i' bands down to $r' \sim 20\,(10\sigma)$. The high quality photometry and characteristics of the survey permit the spectral classification of main-sequence stars to be determined, based on the Hα line strength. The availability of reliably calibrated $(r' - H_\alpha)$ colours permit the spectral classification of most stars, while the $(r' - i')$ colour provides their extinctions, allowing distances to be estimated from the r' measurements. The limiting magnitude in r' permits extinctions to be measured to distances of up ~10 kpc.

IPHAS covers the Galactic latitude range between −5 and 5 deg, and longitude range between 29.52 and 215.49. In this region of the sky, there are 190 known PNe according to the ESO/Strasbourg catalogue (Acker et al. 1992). We were able to extract a reddening for 137 of them from different sources; for 27 PNe, we present the first determinations.

2.1. PN extinctions extracted from the literature

The ESO/Strasbourg catalog provides the H$_\alpha$/H$_\beta$ line ratio for most of the PNe considered here. These data were measured from spectra obtained using two different telescopes: the 1.52 m ESO telescope for the Southern nebulae, and the 1.93 m OHP telescope for the Northern ones. More information about the instruments (photographic plate or CCD) and spectra can be found in Acker et al. (1992, SECGPN), Acker & Stenholm (1987), and Stenholm & Acker (1987). Tylenda et al. (1992) used these SECGPN line intensities to obtain the value of the extinction constant roughly determined for about 900 PNe. In this paper, the visual extinction was obtained from the line ratios by applying the formulae

$$c_\beta = 2.84 \cdot \log\left(\frac{(H_\alpha/H_\beta)}{2.86}\right), \tag{1}$$

$$A_v = 2.15 \cdot c_\beta, \tag{2}$$

which were taken from Fitzpatrick (2004). Here we assumed $R = 3.1$, to be consistent with the method by which the IPHAS extinction curves are built (see Sect. 3).

Other compilations from which c_β was retrieved are Cahn et al. (1992) and in a few cases Stasińska et al. (1992). The latter paper compared the optical and radio extinction determinations, using the same "SECGPN" line fluxes as Tylenda et al. (1992), and adding some other measurements, for a total of 130 PNe. For individual nebulae, these listings where supplemented with data from other papers, where available. In all cases, when the assumed reddening law is reported in a paper, we normalize the published extinction using Eqs. (1) and (2). This is specifically, the case for data in Cahn et al. (1992) and Stasińska et al. (1992). For most of the nebulae, the only available extinction coefficient comes from the Strasbourg catalog, while for a subset there are multiple determinations. For a small number of nebulae, there is a very extensive literature, and in those cases, we selected what we understood to be the most accurate determination of c_β after
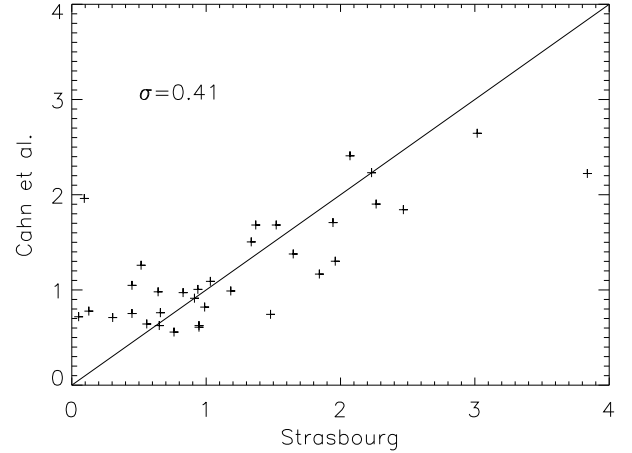
Fig. 1. c_β measurements by by Cahn et al. (1992) plotted against data in Acker et al. (1992). The dispersion is around 0.4 in c_β.

a careful analysis of bibliographic sources. In addition, for some nebulae we also present new optical c_β determinations.

A general rule, in the case of multiple determinations and the absence of other information (the quality of one measurement with respect to another), is to choose the smallest c_β. The main reason is that slit spectra taken at non-negligible zenith distances are often affected by differential atmospheric dispersion which removes blue light leading to an overestimate of the c_β's. Extinction measurements obtained from radio data are free from this effect, but have values that are systematically lower than those determined from the Balmer decrement (Stasińska et al. 1992; Ruffle et al. 2004). To ensure that we have a homogeneous set of measurements, we only consider in this paper c_β obtained from optical measurements.

Finally, to illustrate the differences between extinction determinations by different authors, we show in Fig. 1 the c_β values obtained by Cahn et al. (1992) versus those computed from fluxes in the ESO/Strasbourg catalog. The associated scatter is $\sigma = 0.41$, which shows how critical the choice of the extinction values can be. We note that data from the ESO/Strasbourg catalog are not all of the same quality, those for the northern nebulae ($56 < l < 184$) observed at the OHP being of generally lower quality than those of (mainly southern) nebulae observed at ESO.

2.2. New extinction determinations

Twenty-six PNe considered in this paper (see Tables 1 and 3) were observed at the 2.5 m Isaac Newton Telescope at the Observatorio del Roque de los Muchachos, from August 23 to 30, 1997. The IDS spectrograph was used with its R300V grating, which provides a reciprocal dispersion of 3.31 Å per pixel of the 1k × 1k Tek3 detector, and a spectral coverage from 3700 to 6900 Å. The slit width was 1.5 arcsec projected on the sky, providing a spectral resolution of 6.7 Å. Total exposure times on each nebula varied from a few seconds for the brightest target (NGC 7027) up to one hour for the faintest ones; exposures were split to ensure that both the bright and faint nebular lines were reliably detected without saturation. Several spectrophotometric standards were observed during each night to help perform a relative flux calibration. Data reduction was performed using the package *onedspec* in IRAF.

An additional two PNe (PC 20 and Sa 3-151) were observed with the Dual Beam Spectrograph (DBS, Rodgers et al. 1988) on

Table 1. Distances inferred for the NGC sample.

PNG	Name	A_v				distance [pc]				
		Stras.	Cahn	Stas.	this paper	Others	dC	dVst	dMa	this paper
033.8-02.6	NGC 6741	1.96	1.96	1.93		**1.73**	2047	2260	1700	2680 ± 110
041.8-02.9	NGC 6781		2.09	1.96	2.16 ± 0.11	1.78	699	840	900	<1000
045.7-04.5	NGC 6804		1.85		1.85 ± 0.11	**1.58**	1709	1660	1600	<800
046.4-04.1	NGC 6803	0.96	1.62	1.60		**1.14**	2987	3190	2500	950 ± 130
060.8-03.6	NGC 6853		0.36			0.55	262	400	400	<800
065.9+00.5	NGC 6842	0.96	2.04		**2.08 ± 0.15**		1366		1700	2700 ± 950†
069.4-02.6	NGC 6894		1.80		1.85 ± 0.11	**1.44**	1653	2000	1500	1000 ± 100
074.5+02.1	NGC 6881	3.27	3.62			4.12	2473	3950	1700	n.d.
084.9-03.4	NGC 7027		2.53		2.97 ± 0.46		273	630	700	n.d.
088.7-01.6	NGC 7048	0.65	1.53		**1.20 ± 0.13**	1.27	1598	2220	1200	1000–2000†
089.0+00.3	NGC 7026	1.40	1.34		2.10 ± 0.11	1.69	1902	1940	900	<1500
107.8+02.3	NGC 7354	2.94	3.62		3.99 ± 0.08	**3.23**	1271	1230	800	1000 ± 150

Notes. Columns labelled as "Stras", "Cahn", and "Stas" correspond to the Strasbourg catalog, Cahn et al. (1992), and Stasińska et al. (1992), as well as "dC" and "dVst" are taken from Cahn et al. (1992) and van de Steene & Zijlstra (1994), respectively, while "dMa" from Maciel (1984). "Other" references are given in the text. When significantly different extinction estimates are available, the values reported for the distances are obtained using the absorption values in bold face. Errors are statistical originating in the linear fit to the distance extinction curve, except for NGC 6842 and NGC 7048, where we have also included the errors in the extinction measurement.

May 10 and 14, 2008 by B. Miszalski at the Australian National University 2.3-m telescope. The exposure times were 300 s and 150 s, respectively to achieve a signal-to-noise ratio of about 20 in the peak intensity of H_β. The 1200B and 1200R gratings were used with a slit width of 2″ (positioned at PA = 270 deg) to provide wavelength coverage windows of 4030−5050 Å and 6245−7250 Å at a resolution of ∼1.6 Å (*FWHM*). Data reduction was performed using IRAF and a number of flux standards were observed each night to derive the spectrophotometric response across the separate blue and red spectrograph arms.

3. IPHAS extinction-reddening curves for the PNe

Extinction-distance relationships for the lines of sight toward the sample of 136 Galactic PNe in the IPHAS area were computed with the algorithm MEAD, as described by Sale et al. (2009). MEAD exploits a feature of the IPHAS colour−colour plane, whereby it is possible to accurately determine simultaneously the spectral type of a star and its reddening, avoiding the problems caused by the significant degeneracies that affecting other filter systems and with only a slight dependence on a Galactic model.

Typically, several thousand A to K4 stars in a box of sides 10′, centred on the PNe, were employed in the computation of each relationship. Distances to each star were derived from their apparent magnitude, the MEAD extinction, and the absolute magnitude of the star derived from the MEAD spectral type. The photometric errors were propagated to determine an error in the estimated distance to each star. The stars were then binned by distance, with each bin being at least 100 pc deep, containing at least 8 stars and having a total signal-to-noise ratio in the bin of at least 130. In a small departure from the method described in Sale et al. (2009), the prior probabilities of each luminosity class were determined on a sightline by sightline basis. MEAD evaluates monochromatic extinctions, which can be subsequently converted to A_v using the $R = 3.1$ reddening law of Fitzpatrick (1999).

4. The inversion of distance-extinction curves

The extinction-distance curves obtained are in general linear for a significant range of distances, until they generally flatten out

Table 2. List of PNe with a reported visual extinction more than 1 mag larger than the plateau of the corresponding distance-extinction curve.

PNG	Name	A_v	A_v Plateau	Reference
032.0-03.0	K3-18†	5.56	4.5	1
032.9-02.8	K3-19	4.49	3	1
048.1+01.1	K3-29	6.31	3.5	2
051.0+02.8	WhMe1	7.60	5	1
054.4-02.5	M1-72	4.80	2.5	1, 3
055.2+02.8	He2-432	6.32	4	1
059.9+02.0	K3-39	5.78	3.8	1
064.9-02.1	K3-53	6.25	3.8	1
069.2+02.8	K3-49	4.76	3.4	1
072.1+00.1	K3-57	4.56	3	1
094.5-00.8	K3-83	4.72	3	1
104.1+01.0	Bl2-1	5.76	4	1
110.1+01.9	PM1-339	7.35	6	4
112.5+03.7	K3-88	5	4	1

Notes. The principal source of the H_α/H_β ratio is the ESO/Strasbourg catalog marked as (1) in the column "Reference", while the other sources are: (2) Stasińska et al. 1992; (3) Cahn et al. 1992; and (4) Manchado et al. 1989. (†) K3-18 is a possible symbiotic star.

and reach an asymptotic value once the line of sight leaves the dust layer within the Galactic plane (Fig. 2). Even in the cases where they show a more complex shape, it is generally possible to select a linear region around the point in which we are interested, e.g; the A_v measured for the nebula.

We assume that the measured $A_{v,i}$ are distributed around a true value $A_{v,i}^t = a + bd_i$ following a Gaussian law whose dispersion is σ_A. If so, a least square fit to the selected part of the curve allows us to determine all the needed parameters. Around a point, for each d, the probability-distribution in particular that measures a given A_v is $P(A_v|d)$. The next step is to invert this distribution, i.e; to obtain the probability of finding a distance d for a given $A_{v,i}$: $P(d|A_{v,i})$. We note that

$$P(d|A_{v,i}) = \frac{P(A_{v,i}|d)}{\int P(A_v|d)\mathrm{d}A_v} \quad (3)$$

and using the previous assumptions of linearity and a Gaussian distribution for $P(A_v|d)$, the new distribution for $P(d|A_v)$ is itself

Table 3. Distance to the whole sample of PNe.

PNG	Name	c_β					Distance [pc]				Reference
		Stras. (1)	Cahn (2)	Stas. (3)	this p. (4)	Other (5)	Cahn	Vst.	Ma.	THIS PAPER	
031.7+01.7	PC20	2.51			3.04					>1100	
032.5-03.2	K3-20	1.88								>1100	
032.7-02.0	M1-66	1.39			1.44		3439	5000		>3000	
033.2-01.9	Sa3-151				1.52					3500 ± 300	
035.9-01.1	Sh2-71	1.65	1.38		1.18		997			<1000	
038.7-03.3	M1-69	1.32								3300 ± 500	
040.4-03.1	K3-30	1.67		1.66			6291	6550		>3000	
041.2-00.6	HaTr14	0.56								<1000	
041.8+04.4	K3-15	1.28								>6000	
043.0-03.0	M4-14	1.42					6692	7570	1600	2600 ± 300	
043.1+03.8	M1-65	1.24		**1.23**			6536	6280		3200 ± 900	
043.3+02.2	PM1-276					1.74				1350 ± 100	1
045.4-02.7	Vy2-2	1.94	**1.71**				2159			2300 ± 170	
046.3-03.1	PB9	1.81					4661	3990		3800 ± 450	
047.1+04.1	K3-21	1.15							10500	2700 ± 366	
047.1-04.2	A62		2.07			**0.18**	494		1100	<900	2
048.0-02.3	PB10	2.01					4685	3830		>2000	
048.5+04.2	K4-16	1.51		**1.50**			15127			>5000	
048.7+01.9	He2-429	2.12				**1.87**	3383			1500 ± 600	3
049.4+02.4	He2-428	1.23				**1.14**				1000 ± 100	7
050.1+03.3	M1-67	1.07					682		1000	800 ± 100	
051.0+03.0	He2-430	2.22		2.21			3972			>3000	
051.0-04.5	PC22	0.58								4000 ± 500	
051.9-03.8	M1-73	**0.88**				0.95	4669	4400		2900 ± 500	4
052.2-04.0	M1-74	0.94	1.01	**0.98**			4118	8640		5300 ± 1000	
052.5-02.9	Me1-1	0.05	0.72	0.46		**0.58**	4618			<1000	5
052.9+02.7	K3-31	2.32					3941	6880		800 ± 700	
052.9-02.7	K3-41	1.13					20464	28690		3200 ± 500	
053.3+03.0	A59		1.77		1.61		1412		1800	<1000	
053.8-03.0	A63	1.12			1.09				2700	>8000	
055.1-01.8	K3-43	1.66							1500	>2800	
055.3+02.7	He1-1	2.06								2500 ± 1000	
055.5-00.5	M1-71	1.82		1.80		**2.06**				2900 ± 400	6
055.6+02.1	He1-2	1.86								>3000	
056.0+02.0	K3-35	2.01					3975	6580		<1000	
057.9-01.5	He2-447	2.18					2874			>2000	
058.9+01.3	K3-40	1.72					7068	6490		>3000	
059.0+04.6	K3-34	0.35							5700	<1000	
059.0-01.7	He1-3	1.67								1000 ± 200	
059.4+02.3	K3-37	1.77					7148	7910		2400 ± 400	
060.5-00.3	K3-45	0.84							1900	<1000	
060.5+01.8	He2-440	2.94					3962			>4000	
061.3+03.6	He2-437	1.45				**0.88**				1100 ± 300	7
062.4-00.2	M2-48	2.02				**1.35**	6970		1600	900 ± 200	8
067.9-00.2	K3-52	1.49					2459	7200		2300 ± 200	
068.6+01.1	He1-4	1.77			1.44					>5000	
068.7+01.9	K4-41	1.50					7929	7820		>4000	
068.7+03.0	PC23	1.53					6680	7740		>4000	
068.8-00.0	M1-75				2.11		3190		3100	>4000	
069.2+03.8	K3-46	0.69							3200	1600 ± 100	
069.6-03.9	K3-58	1.34					5635		5700	>3000	
071.6-02.3	M3-35	**2.07**	2.41				1760	4840		2150 ± 150	
075.6+04.3	Anon.20h02	0.01				**0.85**				7000 ± 1300	
076.3+01.1	A69		4.35				4173		300	>4000	
076.4+01.8	KjPn3	0.93								2000 ± 100	
077.5+03.7	KjPn1	1.54								>5500	
077.7+03.1	KjPn2	1.52								3700 ± 400	
078.9+00.7	Sd1	0.11				0.11				<1200	9
084.2-04.2	K3-80	1.18								900 ± 100	
084.9+04.4	A71		1.06				722		900	2800 ± 400	
088.7+04.6	K3-78	0.35					7831	7290		<1200	
089.3-02.2	M1-77	1.23					5496	4880	700	2000 ± 250	
089.8-00.6	Sh1-89	0.99	**0.82**				1941			1350 ± 200	

Table 3. continued.

PNG	Name	c_β					Distance [pc]				Reference
		Stras. (1)	Cahn (2)	Stas. (3)	this p. (4)	Other (5)	Cahn	Vst.	Ma.	THIS PAPER	
091.6-04.8	K3-84	0.51								5200 ± 900	
093.3-00.9	K3-82	0.96					2675	3250		900 ± 130	
093.3-02.4	M1-79	0.13	0.78	**0.77**			2627	3610	1000	4700 ± 800	
093.5+01.4	M1-78	3.02	2.65				700		3100	>2200	
095.1-02.0	M2-49	1.17					2870	6140		>2300	
095.2+00.7	K3-62	2.54					2270	4050		>2500	
096.3+02.3	K3-61	1.32					7334	6510	1100	1000 ± 200	
097.6-02.4	M2-50	0.95	0.63	**0.61**			10028	9280	1500	2700 ± 500	
098.1+02.4	K3-63	1.18	**0.99**				5780		1700	1400 ± 130	
098.2+04.9	K3-60	2.27	1.90	2.59			3887	6210		2000 ± 200	
102.9-02.3	A79		1.33		0.81	**0.36**	1784		1300	1000 ± 160	7
103.7+00.4	M2-52	1.72			1.44		4411		1500	4000 ± 360	
104.4-01.6	M2-53	0.52	1.26		1.06	**0.73**	3737	4940	900	1900 ± 400	
107.4-00.6	K4-57	1.32								4000 ± 1000	
107.4-02.6	K3-87†	1.14					9203	9680		4400 ± 800	
107.7-02.2	M1-80	0.52					5496	4880	1600	1500 ± 200	
111.8-02.8	Hb12			1.35		0.60				<1000	11
112.5-00.1	KjPn8	0.67				**0.42**				1400 ± 100	17
114.0-04.6	A82		0.75				1868		2000	3150 ± 500	
119.3+00.3	BV5-1	1.05		1.31	1.01	**0.82**				3000 ± 400	12
122.1-04.9	A2	0.76	**0.56**	0.34	0.80		3929		3000	1500 ± 150	
126.3+02.9	K3-90	0.83	0.97				5759	5600		<1000	
128.0-04.1	Simeiz22					0.34				<1000	13
130.2+01.3	IC1747	1.48	0.74		1.03		2937	2420		1300 ± 200	
130.4+03.1	K3-92	1.96	1.30		**1.23**		6806			3100 ± 900	
131.5+02.6	A3		1.23	1.22	1.33	**1.23**	2560			5100 ± 500	14
132.4+04.7	K3-93	**1.35**			1.94					<1000	
136.1+04.9	A6		1.39			1.39	958	2240		<1000	
138.8+02.8	IC289	1.03	1.09		1.16		1434	1480		>8000	
142.1+03.4	K3-94	0.91				**0.52**	6507	7740		<1000	15
147.4-02.3	M1-4	2.47	1.84	**1.62**			2988	3390		3300 ± 350	
147.8+04.1	M2-2	1.34	1.50	1.50			4356	3880		>2000	
151.4+00.5	K3-64	0.73								1800 ± 200	
153.7-01.4	K3-65	1.83					10512			3700 ± 300	
160.5-00.5	We1-2					1.44				2500 ± 180	16
163.1-00.8	We1-3					0.70				2700 ± 300	16
167.0-00.9	A8		1.77			**0.68**	1633			5500 ± 1000	2
170.7+04.6	K3-69	1.34					7946		17850	>6000	
178.3-02.5	K3-68	0.80					5945			2200 ± 240	16
181.5+00.9	Pu1					1.03				7000 ± 800	
184.0-02.1	M1-5		1.39	1.38			2922	4940		>4000	
184.6+00.6	K3-70	1.55					12117			>6000	
184.8+04.4	K3-71	1.14								2500 ± 1000	
194.2+02.5	J900	**0.56**	0.64	0.63			2756	3270		4300 ± 650	
197.8-03.3	A14		1.18		1.52	**0.85**	3317			5400 ± 800	10
201.9-04.6	We1-4					0.85				3000 ± 1100	15
204.8-03.5	K3-72					1.06	5119			>4000	15
211.2-03.5	M1-6	1.84	**1.17**	1.83			2648	4290		2000 ± 160	

Notes. The NGC objects listed in the Table 1 and the objects listed in Table 2 are omitted in this table. The columns numbered from 1 to 3 give the values of c_β inferred from H_α and H_β supplied to the Strasbourg catalog (1), from Cahn et al. (1992) (2), from Stasińska et al. (1992) (3). The extinctions obtained in this paper are given in Col. 4. In Col. 5, we present the values obtained in other papers, the corresponding references are: (1) van de Steene et al. 1996; (2) Phillips et al. 2005; (3) Girard et al. 2007; (4) Wesson et al. 2005; (5) Shen et al. 2004; (6) Wright et al. 2005; (7) Rodriguéz et al. 2001; (8) López-Martín et al. 2002; (9) Kazarian et al. 1998; (10) Bohigas 2003; (11) Rudy et al. 1993; (12) Bohigas 2008; (13) Kwitter & Jacoby 1989; (14) Kaler 1983; (15) Bohigas 2001; (16) Kaler et al. 1990; (17) Gonçalves et al. 2009.
The values adopted to obtain the distances are marked in bold-face. If for a PNe no value is shown in bold-face, it means that we find the same results with all of them. Our distance are compared with those obtained by Cahn et al. (1992), van de Steene & Zijlstra (1994), and Maciel (1984).
$^{(†)}$ K3-87 is a possible symbiotic.

Gaussian. We call the central value of this distribution d_A and σ_d the dispersion. It follows that

$$d_A = (A_{v,i} - a)/b, \tag{4}$$

and

$$\sigma_d = \sigma_A/b. \tag{5}$$

In Fig. 2, we show as an example the well-defined extinction curve along the line of sight towards NGC 6894. For this nebula,
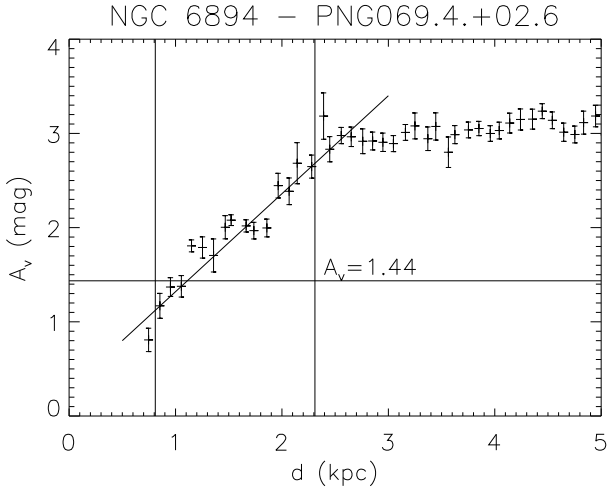
Fig. 2. Extinction law within $10' \times 10'$ around the line of sight toward the NGC 6894. The measured extinction of the nebula is also indicated by the horizontal line, and the two vertical lines delineate the interval in that the law is linear and that we have used to find the corresponding distance to the PN.
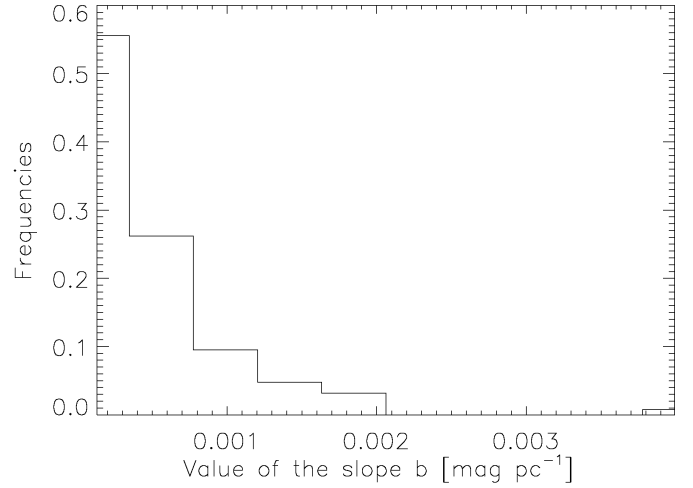

Fig. 3. Distribution of the values of the slope b mag/pc obtained from a linear fit of the interstellar extinction curves. We analysed more than 100 lines of sight corresponding to the known PNe in the IPHAS survey. Almost 80% of the values are distributed between 1.3×10^{-4} and 8×10^{-4}.

the measured extinction value is $c_\beta = 0.67$, or $A_v = 1.44$ (data from Ciardullo et al. 1999). The limits for the selected linear range are 800 and 2300 pc (sensitivity range of the method). The estimated distance is $d = 1000$ pc and the formal standard deviation is $\sigma_d = 150$ pc. We emphasize that the formal σ is only part of the total uncertainty, whose major contribution is due to the error in c_β measurement; we consider other uncertainties in the following section.

To simplify the discussion in the next section about the uncertainty introduced by the inaccuracies in A_v, we fix representative values the parameters b and σ_d. This is achieved by analysing almost two hundred lines of sight. We found a representative mean value for the parameter b of 6.53×10^{-4} mag/pc (Fig. 3), and a typical error in the fitting process of around 10%. A test distance of 2500 pc is also assumed, which is in the middle of the range over which the extinction-distance method is sensitive for the low Galactic latitude coverage that characterizes the IPHAS survey. This range was calculated by taking the mean of the lower and upper limits of the linear interval corresponding to each curve. For the adopted distance, the typical error in the fitting process is around 250 pc. If so, we can express the relative uncertainty in the distance as

$$E = \frac{\sqrt{250^2 + (\sigma_{A_v}/6.53 \times 10^{-4})^2}}{2500}, \tag{6}$$

$$E_{A_v} = \frac{\sigma_{A_v}/6.53 \times 10^{-4}}{2500}, \tag{7}$$

where E is the total uncertainty and E_{A_v} is the contribution of A_v. From the previous formulae for $\sigma_{A_v} = 0.16$ ($\sigma_{c\beta} = 0.077$), we obtain $E_{A_v} \sim 10\%$ and $E \sim 14\%$. We note finally that the previous formulae are exact in the case of purely statistical errors, otherwise they represent a lower limit to the true uncertainty.

5. On the errors

In Sect. 2, we saw how large the difference can be between the c_β values determined for the same nebula by different authors.

The origin of these differences could be systematic errors caused by the instruments or the reduction processes. Unfortunately it is impossible to quantify a priori this effect. However, in the determination of the interstellar reddening, hence of the extinction-distance there are other sources of uncertainty that we discuss below.

5.1. Sources of error relevant to all objects

To determine the visual extinction to a PN, it is common to use the H_α/H_β ratio. However, the literature data often quote only the extinction coefficient c_β. In some cases, the adopted extinction law is also quoted, in such a way that we can convert the c_β's to a common scale, which we assume to be the law given in Fitzpatrick (2004), for $R = 3.1$, for a theoretical ratio $H_\alpha/H_\beta = 2.86$.

The first uncertainty that we consider is that associated with the theoretical H_α/H_β ratio as a function of the electron temperature, for case B. Using Osterbrock (2005) for this ratio, we find that if the electron temperature varies between 8000 and 20 000 K, the largest error that we would make by adopting a ratio of 2.86 is 0.04 dex in c_β, or 0.09 mag in visual extinction. This implies an uncertainty of up to 11% in the distance determination.

The second error source that we consider is the adopted extinction law. Several authors use extinction laws that differ from those adopted in this paper. For example, Stasińska et al. (1992) used the Seaton (1979) law assuming $R = 3.2$, Cahn et al. (1992) used the Whitford (1958) law ($R = 3.2$), while the Howarth (1983, $R = 3.1$) law was used by other authors. The maximum difference between our adopted law occurs when the Cardelli et al. (1989) law is used. We conservatively adopt this difference when the extinction law is not quoted in a paper from which the c_β for a specific PN is adopted. This results in a difference of 15% in c_β, or $\sigma_{A_v} = 0.3$ (for $A_v = 2$), and a contribution to the error in the distance of about 20%.

Another common hypothesis is that the characteristics of the interstellar dust are constant for all lines of sight, and correspond to $R = 3.1$, the mean value of the Milky Way.

Fitzpatrick ([1999](#)) and Fitzpatrick & Massa ([2007](#)) state that for optical wavelengths a single value of R is a good approximation, but R can vary for different lines of sight. Several authors report $R \sim 2$ through the Galactic bulge (Byun [1996](#); Udalski [2003](#); Ruffle et al. 2005) and towards the halo (Larson & Whittet [2005](#)). Based on the study of a sample of PNe, Stasinska et al. ([1992](#)), suggest that for the Galactic plane a more appropriate value is $R = 2.5$. The parameter R may instead be significantly larger if the line of sight crosses a dense dust cloud (due to the generally larger size of the grains). However, we would be unlikely to be able to detect the blue part of the spectrum of PNe (and thus their H_β flux) along such highly extinguished directions. In general, the R value for a particular nebula can in principle be determined if the number of Balmer lines measured with precision is large enough.

Therefore, we cannot exclude there being significant variations in R for our IPHAS sample. Having adopted $R = 3.1$ as a common value, we estimate the error that we make if the true extinction ratio were 2.1 or 5.5 (maximum and minimum values from Fitzpatrick [1999](#); Fitzpatrick & Massa [2007](#)). For the case $R = 2.1$, the Fitzpatrick law gives $A_v = 4.8 \cdot \log(H_\alpha/H_\beta/2.86)$, while we use $A_v = 6.1 \cdot \log(H_\alpha/H_\beta/2.86)$. This results in an overestimate of A_v by some 21%, or $\delta_{A_v} = 0.4$ (for $A_v = 2$). However, in this case the corresponding distance extinction curve is also overestimated by about 15% (Sect. [3](#)). This means that when determining distances these errors partially compensate and the corresponding overestimate of A_v is about 6%, or about 12% for a distance of 2500 pc. For $R = 5.5$, we underestimate A_v by some 33%, but the corresponding extinction curve is also underestimated by 25%, so that a final error is 8% in A_v, or $\sim 14\%$ for the distance.

5.2. Uncertainty originating in object properties

There is additional uncertainty in the hypothesis that the interstellar medium is responsible for all the reddening measured for a PN from the Balmer decrement, in other words, that the PNe are free of internal or circumnebular absorbing dust (for a review see Barlow [1983](#)). This hypothesis is in general supported by the study of Köppen ([1977](#)), which, assuming that in a planetary nebula the dust and gas components are well mixed, finds that the nebular dust optical depth is very small ($\tau < 0.05$), for a dust/gas ratio of around 10^{-3}. However, this could be too simple a picture, and in this original work there were also some PNe (6 out of a total of 21) with evidence of associated extinction. The effect is probably negligible for standard, elliptical PNe (Barlow [1983](#)), but could be more significant for particular nebular morphologies, such as that of bipolar PNe from massive progenitors (e.g. Corradi & Schwarz [1995](#)), which may have massive neutral equatorial envelopes. There is some evidence in the literature that this might be the case.

The most studied example of the latter type is NGC 7027. Osterbrock ([1974](#)) estimated a maximum internal absoption of 0.6 mag. Woodward et al. ([1992](#)) suggested that the obscuring dust lies in a shell or disc external to the ionized gas, and Bieging et al. ([2008](#)) found variations in c_β from 0.8 to 2.4. A variation in A_v was also measured for NGC 650-1 between the SW and NE limits of the central emission bar by Ramos-Larios et al. ([2008](#)). Other type-I bipolar nebulae, such as Sh 2-71, K 3-94, K 4-55, and M 1-75, appear to have some (generally modest) extinction variations across their structures (Bohigas [1994](#), [2001](#)). Extreme variations are clearly found for NGC 6302 and NGC 6537 (Matsuura et al. [2005a](#),b).

There are also a few indications of associated extinction for non-bipolar morphologies[1]. In this context, an interesting object is NGC 6741, for which Sabbadin et al. ([2005](#)) find a circumnebular neutral halo generated during a recombination phase following the fading of the central star. This halo was estimated to be responsible for 10−20% of the measured total c_β. The Helix nebula (NGC 7293) seems to be a very complex object in which dust, ionized, and molecular gas cohabit (Speck et al. [2002](#)). Dense knots in a PN could also evolve into absorbing filaments, as reported by O'Dell et al. ([2003](#)) for the bipolar PN IC 4406.

For NGC 6781, Mavromatakis et al. ([2001](#)) provide a 2D Balmer decrement map, finding variations in H_α/H_β ranging from 5.6 to 7. Though smaller, similar structures are also visible in a similar map obtained for Menzel 1 by Monteiro et al. ([2005](#)).

To summarize, in some cases care has to be taken when determining the interstellar extinction, especially for particular geometries (bipolar). However, because of the small number of studies it is difficult to estimate the percentage of objects belonging to these categories whose interstellar extinction could be wrongly estimated. In any case, the number of bipolar PNe is 15% of the total number of planetary nebulae (Corradi & Schwarz [1995](#)), and from this subsample significant unrecognized errors are probable only for distant, spatially unresolved objects. We can conclude that only a small fraction of our total sample will be affected by this kind of uncertainty in the estimate.

Concluding, at present the major contribution to the uncertainty in the distances originates in the A_v's error measurements. For two nebulae, NGC 6842 and NGC 7048, our own measurements allow us to estimate these errors. Combining it with the statistical fitting error leads to a final uncertainty in the distance in about 35%.

6. Distance determinations for the NGC sample

To minimize the uncertainties, we infer the distances for a sample of very well known PNe in the IPHAS area, shown in Table [1](#).

The first PN is NGC 6741 (PNG 033.8-02.6, Fig. [4](#)), which, as discussed in the previous section, was found to have nonnegligible internal extinction by Sabbadin et al. ([2005](#)). We use the interstellar value given in the same paper to determine its distance. The reported error in the distance comes from the statistical σ_d. This also applies to the other PNe in this section, except for NGC 6842 and NGC 7048 as discussed later.

For NGC 6781 (PNG 041.8-02.9, Fig. [4](#)) we derive a distance of smaller than 1000 pc, by adopting all the reported values of A_v, from the minimum value inferred by Mavromatakis et al. ([2001](#)) to the maximum value obtained in this paper. We cannot be more precise since the curve is not determined within this range. However, the result is in line with that of Schwarz & Monteiro ([2006](#)), who found a distance of 750 pc using 3D photoionization modeling.

For NGC 6804 (PNG 045.7-04.5, Fig. [4](#)), we use the determination of A_v obtained by Ciardullo et al. ([1999](#)), using Hubble images. The graph was transferred to the Fitzpatrick law ($R = 3.1$), which is our adopted law for the interstellar extinction. In this case, the inferred distance is <800 pc, while from our measurement of c_β and the corresponding error we estimate 850 ± 70 pc. This is a factor of 2 smaller than the statistical distances reported by Cahn et al. ([1992](#)) and

---

[1] Note that morphological misclassification my be caused for a fraction of PNe by orientation effects: see Manchado ([2004](#)).
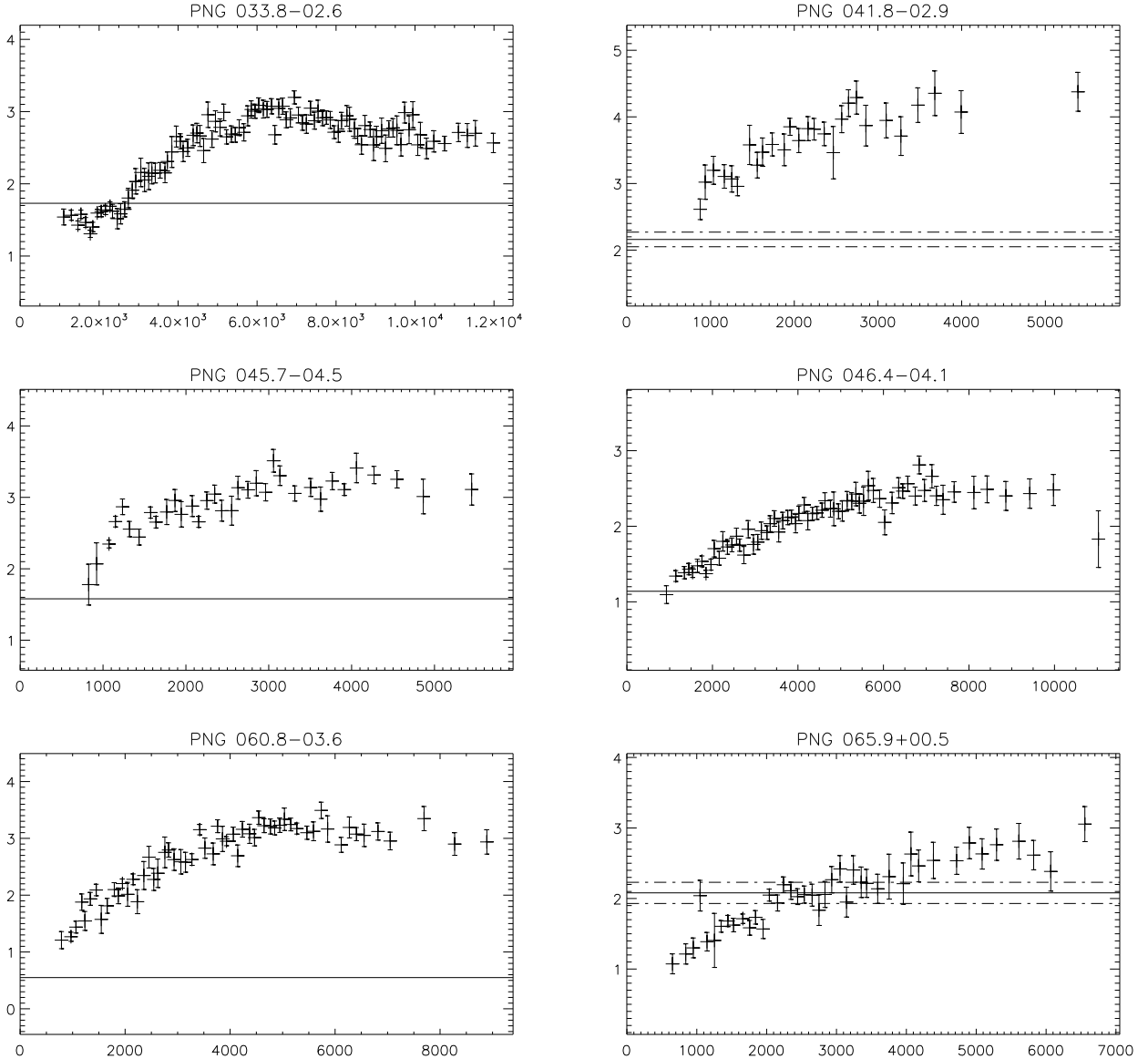
Fig. 4. We present the extinction distance curves for the first 6 nebulae reported in Table 1. The abscissae are in pc, the ordinates in visual magnitudes, and the horizontal lines represent the visual extinction corresponding to each nebula, as discussed in the text. The short dash-long dash lines represent the 1-σ error associated with our A_v measurement presented in Table 1.

van de Steene & Zijlstra (1994). The error in the statistical scales is typically 30% (1σ), so that these values do not exclude the much shorter (and with a smaller uncertainty) distance found here. In support of the smaller distance, we also note that a drawback of the extinction method is a tendency to overestimate distances. Moreover, this is a bipolar nebula for which because of the measured extinction may be significantly higher than the interstellar component because of absorbing structure associated with the PN.

In our method, the only circumstance in which we can underestimate the distance is if the parameter $R > 3.1$. This can occur when the line of sight intersects a dense molecular cloud (a rare event). The map of dense molecular clouds in the Galaxy given by Hartmann & Thaddeus (2001) does not contain any clouds at these coordinates. We therefore recommend the use of our estimated range <800 pc, which is also close to the estimate of 870 pc by Frew (private communication, Frew et al. 2010, in preparation), based on a relationship between size and surface brightness for PNe.

For NGC 6803 (PNG 046.4-04.1, Fig. 4), using the extinction value determined by Peimbert & Torres-Peimbert (1987) ($c_\beta = 0.53$, $A_v = 1.14$), we infer a distance of 950 pc, again smaller than half the previously reported estimates. Even using the much higher values of c_β presented by Cahn et al. (1992), we obtain smaller distances (2100 ± 300 pc) than those previously reported.

For the nearby nebula NGC 6853 (PNG 060.8-03.6, Fig. 4), a parallax measurement was performed by Benedict et al. (2003) yielding a distance of 417^{+49}_{-65} pc and a visual extinction coefficient tabulated in the column labeled "Others" of Table 1. In this case, the nebula is outside of the sensitivity range of our method and we can provide only an upper limit to the distance.

For NGC 6842 (PNG 065.9+00.5, Fig. 4), there is little information in the literature. From our own measurement obtained at the 2.5 m Isaac Newton Telescope on La Palma, we determine an extinction measurement that is clearly higher than that inferred by adopting line fluxes from the Strasbourg catalog. Observations imply a distance of 2700 ± 950 pc. The error in
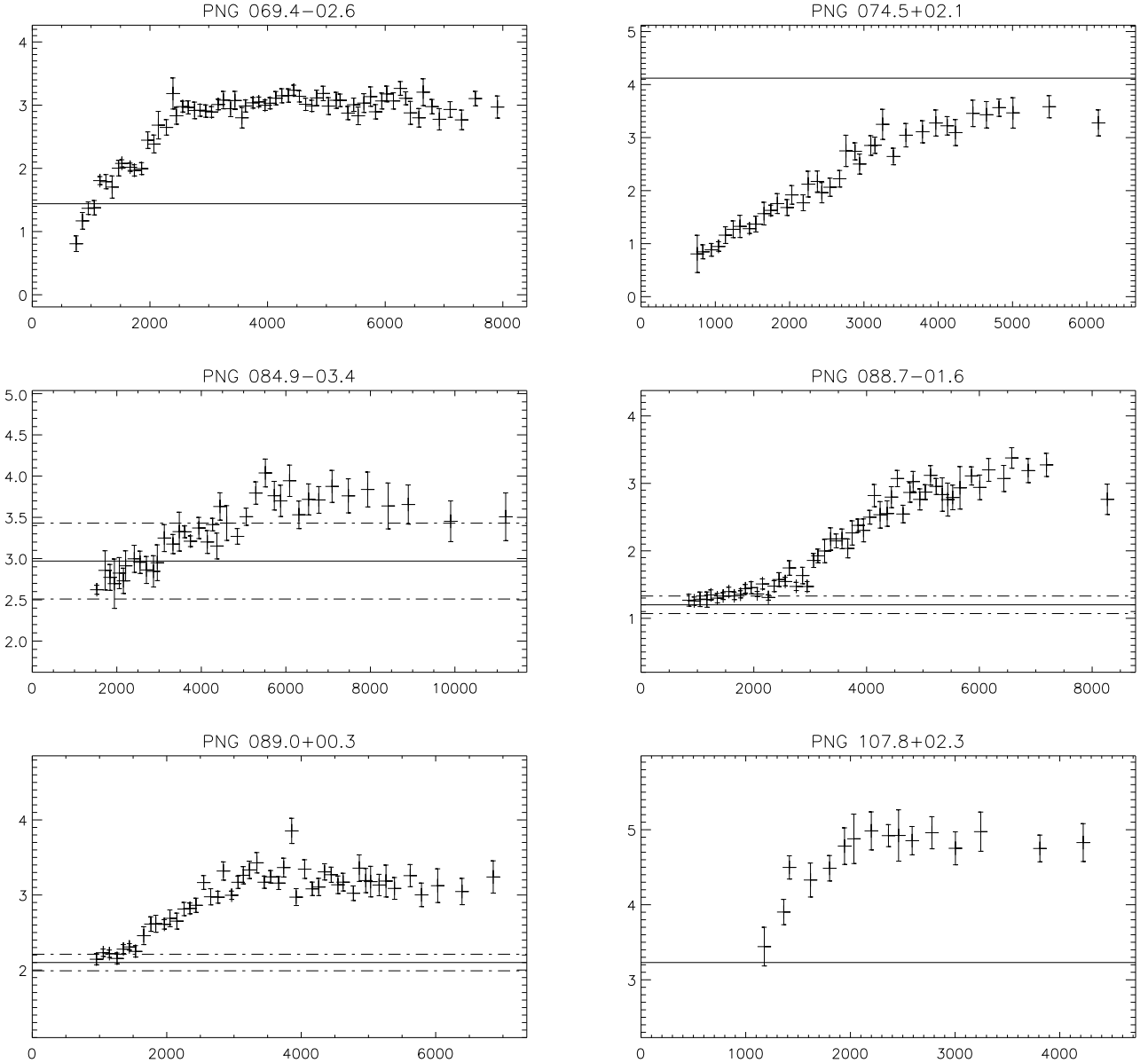
Fig. 5. Extinction-distance curves for the second group of six nebulae presented in Table 1. For all graphics, the abscissae are in pc, the ordinates, in visual magnitudes. The horizontal lines represent the visual extinctions corresponding to the nebulae considered in the text. The short dash-long dash lines represent the 1-σ error associated with our A_v measurement presented in Table 1.

the distance has been calculated by taking into account the fitting $\sigma_d = 749$ pc, the error in the extinction measurement 0.15, and the slope of the curve, $b = 2.6 \times 10^{-4}$ pc/mag.

NGC 6881 (PNG 074.5+02.1, Fig. 5) is a quadrupolar young nebula (Guerrero & Manchado 1998) suggested by Sabbadin et al. (2005) to have been produced by a massive progenitor and presently in a similar recombination phase to NGC 6741. If so, it is possible that c_β overestimates the interstellar extinction and thus the distance using the extinction method, which would then be greater than 4000 pc using the very high absorption reported in column "Others" (Kaler & Kwitter 1987), as well as the value obtained from the Strasbourg catalog. For this reason, we do not quote a distance in Table 1.

NGC 6894 (PNG 069.4-02.6, Fig. 5) and NGC 7048 (PNG 088.7-01.6, Fig. 5) are morphologically simpler. The A_v of NGC 6894 is taken from Ciardullo et al. (1999). The extinction coefficient determinations for NGC 7048 are more contradictory. By adopting the lowest one, we found that this is a nearby nebula

(<1000 pc). However, any distance closer than 1000 pc makes the central star absolute magnitude so faint that by using a standard evolutionary track we infer an age of $\gg 10^5$ yrs for the PN, so it is probably more distant. Assuming instead the c_β obtained by our measurement, which agrees with the value in Sabbadin et al. (1987) ($A_v = 1.27$), we found a distance of between 1000 and 2000 pc.

NGC 7027 (PNG 084.9-03.4, Fig. 5) is the clearest case of strong internal absorption, as discussed in Sect. 5. Given the difficulty in estimating its exact amount as a function of the position at which c_β is measured, no extinction distance is given in Table 1 for this nebula.

NGC 7026 (PNG 089.0+00.3, Fig. 5) is a bipolar nebula with a low extinction coefficient. Using any of the extinction values in Table 1, we found a distance <1500 pc.

Finally, Benetti et al. (2003) propose NGC 7354 (PNG 107.8+02.3, Fig. 5) as a probable recombining nebula in its first phase, as derived from a detailed study of

NGC 6818. Using the Feibelman (2000) extinction data and extrapolating the extinction-distance curve to low distances, we found a possible distance of about 1000 pc.

7. Determination of distances for whole sample

We now present distances for 64 other planetary nebulae in the area of sky covered by IPHAS. For an additional 29 objects, only a lower limit to the distance could be obtained. For 17 PNe, we found an upper limit, as given in Table 3. We adopt a distance upper limit when the measured extinction to the nebula is smaller than the first point on the corresponding distance-extinction curve. A distance lower limit is defined when the visual extinction to the nebula lies on the plateau of the interstellar extinction curve. For multiple determinations of c_β, the source of the adopted value is reported in bold-face. For upper and lower limits, if no indication is given it means that the same conclusion holds for all tabulated c_β's. The errors in the distances given in Table 3 are the fitting errors σ_d.

For the 14 PNe listed in Table 2, we could not estimate the distances because the measured extinction was too far above the interstellar extinction plateau. According to the discussion of Sect. 2.1 and the results presented in Fig. 1, we assume that we know c_β with the uncertainty $\sigma = 0.41$, which is 0.88 mag in A_v, for the data extracted from Acker et al. (1992).

We therefore consider all PNe with a visual extinction more than 0.88 mag higher than the plateau value to be "above" the plateau. Assuming these nebulae to be above the plateau is a zero order hypothesis, because the measured extinctions are not a homogeneous set of measurements and using a common sigma is not rigorous. However, the PNe listed in Table 2 form a sample for future detailed studies, to understand whether the discrepancy with the reddening-distance curve is caused by measurement errors, or if the nebulae have peculiar physical conditions that affect the determination of c_β (e.g. very high densities that introduce optical thickness effects), whether they are misclassified objects (symbiotic stars, nebulae around young stars, etc.), or whether there is indeed a non-negligible amount of reddening associated with the PNe themselves and not of interstellar origin.

The inferred distances are compared in Fig. 6 with those of Cahn et al. (1992), based on a modified Shklovsky-Daub method, of van de Steene & Zijlstra (1994), based on a correlation between radio continuum brightness temperature and radius, and of Maciel (1984), based on a mass-radius relationship established from selected electron densities and distances. It is interesting to note that the first two methods seem to provide larger distances than our extinction method, while the latter seems to provide shorter distances. The spread in these graphs is 4.0 kpc (Cahn et al. 1992, 39 objects), 6.6 kpc (van de Steene & Zijlstra 1994, 23 objects), and 2.5 kpc (Maciel 1984). It therefore seems that the distances found by Maciel are in closer agreement with ours than those from the other authors. However, the small number of objects considered (16 PNe, nine of which are at an estimated distance smaller than 2 kpc), prevents any conclusion to be drawn about the present sample.

Comparison with other distance scales would be very valuable to help us understand this problem. A detailed comparison with distances determined via the relation between size and H$_\alpha$ surface brightness (Frew et al. 2006; Frew 2008) will be presented in a future paper, after the global photometric calibration of the IPHAS survey becomes available.
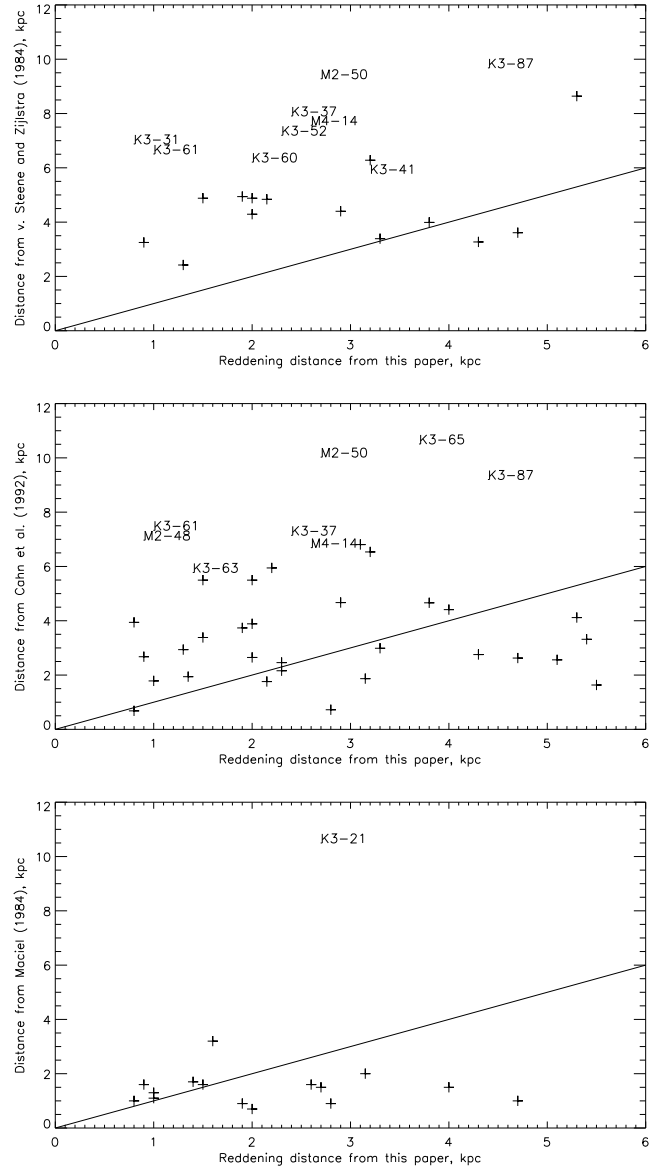
Fig. 6. Comparison between the reddening distance and the statistical determination. The straight line is the 1:1 locus, the statistical distance for the nebulae over the line is greater than that inferred by the extinction. Those PNe for which the difference between the two inferred distances is larger than 4 kpc are labeled in the figure.

8. Conclusions

We have discussed the extinction-distance method for determining distances to PNe, motivated by the opportunity provided by the IPHAS survey with its wide application in the Galaxy.

The technique has been presented and the derivation of the distance and its error placed on a formal mathematical basis. We have derived a mean value of the slope $b = 6.53 \times 10^{-4}$ mag/pc for the galactic extinction distance curve, valid for the analysed region of the sky.

The numerical and physical problems affecting the measurement of the interstellar extinction toward a PN have been discussed. These problems add error to the unavoidable measurement, the effects of an incomplete knowledge of the physics of interstellar dust through the Galaxy and inside PNe, and have to be taken into account every time the method is applied.

In spite of these uncertainties, which will need to be fully addressed in future, we have computed extinction distances for a sample of 70 PNe, which is the largest sample of Galactic PNe to which the technique has been applied. In optimal conditions, when the extinction measurements of the PNe are of good quality and the lines of sight are well behaved in terms of their associated distance-extinction maps, the errors in the PN distances can be as small as 20%, which is a very promising result for a wider application of the method. Unfortunately this is not the common situation for the current data set. As previously mentioned, the uncertainty in the visual extinction for the whole set of nebulae is $\sigma = 0.88$, which implies much larger errors in the distances. For a subsample of the PNe considered, extinction is more precisely measured, and for the two cases for which we could determine the associated error, an uncertainty of 35% in the distance is estimated. This can be taken as a figure to be associated with PNe for which good spectroscopic data exist. A main message of this study is that a careful determination of the nebular extinction is mandatory to limit the errors in such a way that reliable distances can be obtained for individual objects. In this respect, our plan is to improve the extinction measurements for a significant sample of Galactic PNe.

We have compared these new extinction distances with other statistical methods. Some of the methods considered (Cahn et al. 1992; and van de Steene & Zijlstra 1994) provide distances that are generally larger than our determinations, and in general the spread between our measurements and the statistical determinations is quite high. This emphasizes the large 1-σ dispersion in the statistical distances, and the dangers in relying on the determination of a statistical distance to a PN without considering the particular characteristics of a given nebula.

We conclude, by highlighting that the analysis in this paper demonstrates the improved potential of the extinction method provided by the availability of surveys such IPHAS, which provide precise photometric data across large areas of sky. This opens the possibility of making a significant step forward in the calibration of the PN distance scale in the Galaxy, and in our understanding of important issues such as the properties of the dust distribution within the Galactic disc, and the possible importance of dust associated with PNe.

References

Acker, A. 1978, A&AS, 33, 367
Acker, A., & Stenholm, B. 1987, ESO Messenger, 48, 16
Acker, A., Marcout, J., Ochsenbein, F., Stenholm, B., & Tylenda, R. 1992, (SECGPN) Strasbourg – ESO catalogue of galactic planetary nebulae, Garching: European Southern Observatory
Barlow, M. 1983, Proc. IAU Symp., 103, 105
Benedict, G. F., McArthur, B. E., Fredrick, L. W., et al. 2003, ApJ, 126, 2549
Bensby, T., & Lundström, I. 2001, A&A, 374, 599
Benetti, S., Cappellaro, E., Ragazzoni, R., Sabbadin, F., & Turatto, M. 2003, A&A, 400, 161
Bieging, H., Boley, P. A., Latter, W. B., & Tielens, A. G. G. M. 2008, ApJ, 676, 390
Bohigas, J. 1994, A&A, 288, 617
Bohigas, J. 2001, RMxAA, 37, 237
Bohigas, J. 2003, RMxAA, 39, 149
Bohigas, J. 2008, ApJ, 674, 954
Byun, Y.-I. 1996, ChJPh, 34, 1113
Cahn, J. H., Kaler, J. B., & Stanghellini, L. 1992, A&AS, 94, 399
Cardelli, J. A., Clayton, G. C., & Mathis, J. S. 1989, ApJ, 345, 245

Christianto, H., & Seaquist, E. R. 1998, AJ, 115, 2466
Ciardullo, R., Bond, H. E., Sipior, M. S., et al. 1999, AJ, 118, 488
Corradi, R. M. L., & Schwarz, H. E. 1995, A&A, 293, 871
Cuesta, L., Phillips, J. P., & Mampaso, A. 1996, A&A, 313, 243
Drew, J. E., Greimel, R., Irwin, M. J., et al. 2005, MNRAS, 362, 753
Feibelman, W. 2000, PASP, 112, 861
Fitzpatrick, E. L. 1999, ASP, 63, 75
Fitzpatrick, E. L. 2004, ASPC, 309, 33
Fitzpatrick, E. L., & Massa, D. 2007, ApJ, 663, 320
Frew, D. J. 2008, unpublished Ph.D. Thesis, Macquarie University
Frew, D. J., Parker, Q. A., & Russeil, D. 2006, MNRAS, 372, 1081
Gathier, R., Pottasch, S. R., & Pel, J. W. 1986, A&A, 157, 171
Girard, P., Köppen, J., & Acker, A. 2007, A&A, 463, 265
Gonçalves, D. R., Mampaso, A., Corradi, R. L. M., & Quireza, C. 2009, MNRAS, 398, 2166
Guerrero, M. A., & Manchado, A. 1998, ApJ, 508
Hartmann, D. T. M., & Thaddeus, P. 2001, ApJ, 547, 792
Howarth, I. D. 1983, MNRAS, 203, 301
Kaler, J. B. 1983, ApJ, 271, 188
Kaler, J. B., & Kwitter, K. B. 1987, PASP, 99, 952
Kaler, J. B., Shaw, R. A., & Kwitter, K. B. 1990, ApJ, 359, 392
Keler, J. B., Kwitter, K. B., Shaw, R. A., & Browing, L. 1996, PASP, 108, 980
Kazarian, M. A., Parsamian, S., & Parrao, L. 1998, Astrophys., 41, 239
Köppen, J. 1977, 56, 189
Kwitter, K. B., & Jacoby, G. H. 1989, AJ, 98, 2159
Larson, K. A., & Whittet, D. C. B. 2005, AJ, 623, 897
López-Martín, L., López, A., Esteban, C., et al. 2002, A&A, 388, 652
Lutz, J. H. 1973, ApJ, 181, 135
Maciel, W. J. 1984, A&AS, 55, 253
Manchado, A. 2004, ASPC, 313, 3
Manchado, A., Riera, A., Mampaso, A., García Lario, P., & Pottasch, S. R. 1989, RMxAA, 18, 182
Matsuura, M., Zijlstra, A. A., Gray, M. D., Molster, F. J., & Waters, L. B. F. M. 2005a, MNRAS, 363, 628
Matsuura, M., Zijlstra, A. A., Molster, F. J., et al. 2005b, MNRAS, 359, 383
Mavromatakis, F., Papamastorakis, J., & Paleologou, E. V. 2001, A&A, 374, 280
Monteiro, H., Schwarz, H. E., Gruenwald, R., Guenthner, K., & Heathcote, S. R. 2005, ApJ, 620, 321
O'Dell, C. R., Balick, B., Hajiam, A. R., Henney, W. J., & Burkert, A. 2003, RMxAA Ser. Conf., 15, 29
Osterbrock, D. E. 1974, PASP, 86, 609
Osterbrock, D. E. 2005, Astrophysics of gaseous nebulae and active galactic nuclei (University Science Books), 73
Peimbert, M., & Torres-Peimbert, S. 1987, RMxAA, 15, 117
Peña, M. 2005, RMxAA, 41, 423
Peña, M., Stasińska, G., & Medina, S. 2001, A&A, 367, 983
Phillips, J. P., Cuesta, L., & Kemp, S. N. 2005, MNRAS, 357, 548
Pollacco, D. L., & Ramsay, G. 1992, MNRAS, 254, 228
Ramos-Larios, G., Phillips, J. P., & Cuesta, L. 2008, MNRAS, 391, 52
Rodgers, A. W., Conroy, P., & Bloxham, G. 1988, PASP, 100, 626
Rodriguéz, M., Corradi, R. L. M., & Mampaso, A. 2001, A&A, 377, 1042
Rudy, R. J., Rossano, G. S., Erwin, P., Puetter, R. C., & Feibelman, W. A. 1993, AJ, 105, 1002
Ruffle, P. M. E., Zijlstra, A. A., Walsh, J. R., et al. 2004, MNRAS, 353, 796
Sabbadin, F., Cappellaro, E., & Turatto, M. 1987, A&A, 182, 305
Sabbadin, F., Benetti, S., Cappellaro, E., Ragazzoni, R., & Turatto, M. 2005, A&A, 436, 459
Sale, S. E., Drew, J. E., Unruh, Y. C., et al. 2009, MNRAS, 392, 497
Schwarz, H. E., & Monteiro, H. 2006, ApJ, 648, 430
Seaton, M. J. 1979, MNRAS, 187, 73
Shen, Z.-X., Liu, X.-W., & Danziger, I. J. 2004, A&A, 422, 563
Speck, A. K., Meixner, M., Fong, D., et al. 2002, AJ, 123, 346
Stasińska, G., Tylenda, R., Acker, A., & Stenholm, B. 1992, A&A, 266, 486
Stenholm, B., & Acker, A. 1987, Proc. Frascati Workshop Planetary and Proto-planetary Nebulae from IRAS to ISO, ed. Praite-Martínez, 25
Tylenda, R., Acker, A., Stenholm, B., & Köppen, J. 1992, A&AS, 95, 337
Udalski, A. 2003, ApJ, 590, 284
van de Steene, G. V., & Zijlstra, A. A. 1994, A&A, 108, 485
van de Steene, G. C., Jacoby, G. H., & Pottasch, S. R. 1996, A&AS, 118, 243
Warner, J. W., & Rubin, V. C. 1975, ApJ, 198, 593
Wesson, R., Liu, X.-W., & Barlow, M. J. 2005, MNRAS, 362, 424
Wright, A., Corradi, R. L. M., & Perinotto, M. 2005, A&A, 436, 967
Woodward, C. E., Pipher, J. L., Forrest, W. J., Moneti, A., & Shure, M. A. 1992, ApJ, 385, 567